Robust and Self-Cleaning Electrochemical Production of Periodate

Camila M. Kisukuri[+],[a] Roland Jan-Reiner Bednarz[+],[a] Christopher Kampf,[a] Sebastian Arndt,[a] and Siegfried R. Waldvogel*[a]

Periodate, a platform oxidizer, can be electrochemically recycled in a self-cleaning process. Electrosynthesis of periodate is well established at boron-doped diamond (BDD) anodes. However, recovered iodate and other iodo species for recycling can contain traces of organic impurities from previous applications. For the first time, it was shown that the organic impurities do not hamper the electrochemical re-oxidation of used periodate. In a hydroxyl-mediated environment, the organic compounds form CO_2 and H_2O during the degradation process. This process is often referred to as "cold combustion" and provides orthogonal conditions to periodate synthesis. To demonstrate the strategy, different dyes, pharmaceutically active ingredients, and iodine compounds were added as model contaminations into the process of electrochemical periodate production. UV/Vis spectroscopy, NMR spectroscopy, and mass spectrometry (MS) were used to monitor the degradation of organic molecules, and liquid chromatography-MS was used to control the purity of periodate. As a representative example, dimethyl 5-iodoisophthalate (2 mM), was degraded in 90, 95, and 99 % while generating 0.042, 0.054, and 0.082 kilo equiv. of periodate, respectively. In addition, various organic iodo compounds could be fed into the periodate generation for upcycling such iodo-containing waste, for example, contrast media.

Introduction

The EU aims for Europe being climate neutral by 2050. This ambitious goal requires electrification of many industrial processes. Electro-organic synthesis may contribute to this goal substantially because it provides sustainable access to a growing number of compounds while allowing for controlled degradation of others (i.e., pollutants and waste products).[1–9] Electro-organic reactions provide numerous advantages compared to conventional synthetic approaches.[5,10–15] For example, hazardous and stoichiometric chemical redox reagents can be substituted directly by electricity derived from regenerative energy sources. This increases atom economy and lowers waste production for the desired reaction.[5,10,11,16,17] Further advantages are the improvement of safety and milder reaction conditions. In total, this sustainable approach can pay off.[18]

Batch-type electrolysis cells, typically used in research laboratories, limit the scale-up of electrochemical reactions to a technical scale due to low space-time yields. One potential approach to practically and economically overcome this scalability issue is the operation of the electrolysis reactions under continuous-flow conditions.[19,20] Advantages of this approach are the higher energy efficiency due to smaller interelectrode distance (narrow gap) and the improved selectivity due to higher electrode surface/volume ratio in a flow electrolyzer.[21–26] Therefore, efficiencies of mass, energy, and electron transfer can be enhanced significantly.[27–30]

Periodate represents a strongly oxidizing hypervalent iodine species, able to facilitate a large scope of oxidative transformations in organic synthesis.[31,32] Prominent examples include cleavage of carbon–carbon bonds of a variety of 1,2-difunctionalized alkanes,[33] iodinations of alkenes and arenes,[34,35] oxidation of polysaccharides, as well as Malprade and Lemieux–Johnson oxidations.[36,37] Periodate is thus widely used in the synthesis of active pharmaceutical ingredients (APIs) (Figure 1).[38–40]

Commonly, periodate can be produced from $NaIO_3$, which can be synthesized from iodine and excess $NaClO_3$.[41] However, due to the high costs related to purification after the synthetic process or protocols with low efficiencies, traditional methods are reported as expensive.[42,43] Additionally, they involve dangerous and toxic reagents and show poor atom efficiency.[44,45]

An electrochemical approach is generally preferred over a chemical method.[46] Among the large variety of electrosynthesis pathways, oxidative reactions can be carried out at lead dioxide (PbO_2) or boron-doped diamond (BDD) anodes.[44] Among these two, PbO_2 has often been used preferentially as the anode material, due to electro-catalytic effects and its high over-potential for oxygen evolution in aqueous media.[47] Nevertheless, at high positive potentials PbO_2 electrodes can form

[a] Dr. C. M. Kisukuri,+ R. J.-R. Bednarz,+ Dr. C. Kampf, Dr. S. Arndt, Prof. Dr. S. R. Waldvogel
    Department of Chemistry
    Johannes Gutenberg University Mainz
    Duesbergweg 10–14, 55128,
    Mainz (Germany)
    E-mail: waldvogel@uni-mainz.de

[+] These authors contributed equally to this work.
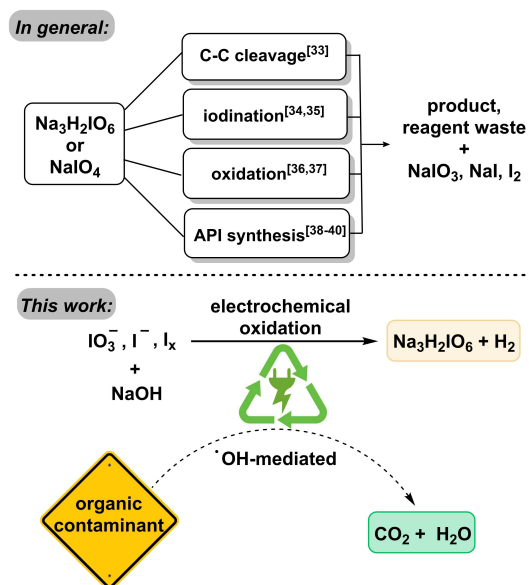
Figure 1. Examples of reported use of periodate in comparison to the use of periodate as platform oxidizers and elimination of organic impurities (this work).

"mud", increasing energy consumption and product contamination.[48,49]

In the last decades, the research for innovative electrode materials has focused on BDD anodes. Favorable properties of BDD electrodes include: (i) wide range of acceptable solvents; (ii) low background currents; (iii) reduced fouling; (iv) no corrosion at high temperatures; and (v) biocompatibility.[50–54]

Janssen and Blijlevens reported the use of BDD anodes for the production of periodate, mostly based on expensive lithium salts.[48] Recently, we established the sodium periodate production using electro-organic synthesis in a flow electrolyzer.[55] In this protocol, alkali iodides were used as the least expensive commercial source of iodine and caustic conditions were chosen to achieve a high current efficiency of 84%, while avoiding the precipitation of iodine. Highly toxic anti-reducing agents could be omitted using a divided cell setup employing a Nafion membrane. The electrochemically produced *para*-periodate has been successfully demonstrated to efficiently degrade lignin,[56] and to achieve the final oxidative step in the synthesis of levetiracetam and sulfoximines.[57,58]

Here, we demonstrate that electrolyses to the periodate platform oxidizer are highly robust against the presence of several organic contaminants (i.e., dyes, APIs, and other iodine compounds). Mineralization of these impurities is not harming the oxidative recycling of periodate. As shown previously, the formation of periodate occurs via hydroxyl radicals, which can also degrade and mineralize the organic impurities.[59–61] In this study, 8 different organic dyes, 3 contrast media, and 8 different iodine compounds were tested as impurities and shown to degrade during periodate recycling, as verified by UV/Vis spectroscopy and mass spectrometry (MS). Iodo compounds (e.g., from industrial processes) could even enhance the periodate yield by upcycling. Degradation of the compounds was

measured in the scale of kilo equivalents of *para*-periodate in a co-production process. Dimethyl 5-iodoisophthalate was degraded with 90, 95, and 99% efficiency, while generating 0.042, 0.054, and 0.082 kilo equiv. of *para*-periodate, respectively. Commonly, all investigated examples were degraded to 99%, while consuming 0.082–52.4 kilo equiv. of periodate.

Results and Discussion

General flow electrolyzer for periodate production

At first, the platform developed for the synthesis of sodium periodate was set in operation. The parameters were adjusted to the best reaction conditions. This includes the use of a divided flow electrolysis cell composed of a stainless-steel cathode (4×12 cm^2) and a BDD anode (4×12 cm^2). A Nafion membrane was used to separate the compartments. The electrochemical reaction parameters were adjusted to a galvanostatic reaction using a constant current density of 312 mA cm^{-2} ($I = 15$ A). The aqueous anolyte (4 M NaOH; 0.21 M Na$_3$H$_2$IO$_6$) and aqueous catholyte (4 M NaOH) solutions were pumped through the electrolyzer with a flow rate of 7.5 L h^{-1}. A complementary pump was used to keep the volume of catholyte and anolyte constant. Here, a rate of 0.3 mL min^{-1} was used. Also, a cryostatic bath circulator, for controlling the temperature of the electrolyzer was employed. To test the degradation of the organic contaminants, selected compounds were added into the anodic compartment. Figure 2 schematically illustrates the setup to re-oxidize periodate and degrade
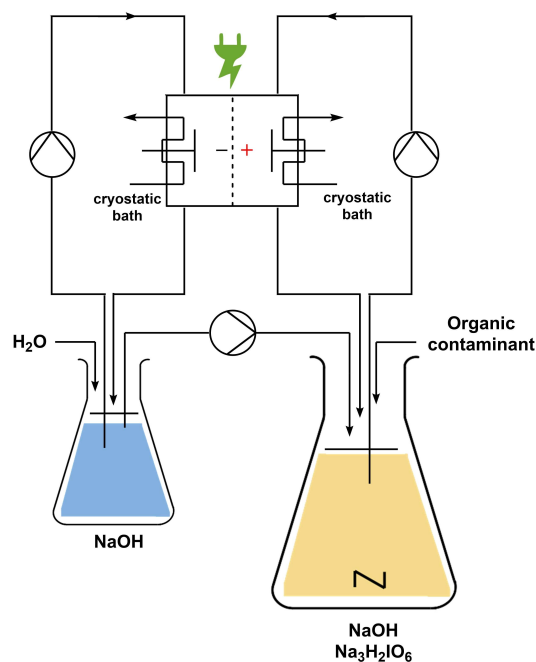
Figure 2. General scheme for the periodate platform oxidizer: self-cleaning electrochemical re-oxidation to periodate following the degradation of organic compounds; cooling cryostat pump.

ChemSusChem

Research Article
doi.org/10.1002/cssc.202200874

**Chemistry
Europe**
European Chemical
Societies Publishing

organic molecules. A detailed set of pictures of the system is displayed in the Supporting Information (Figures S1 and S2).

In general, the established flow system proved to be robust, not showing leaks or clogging after the re-oxidation and degradation experiments.

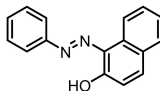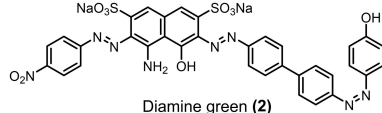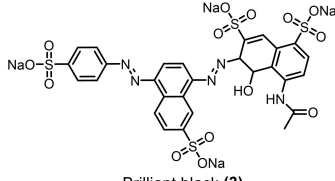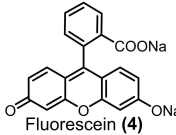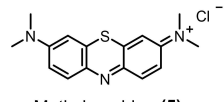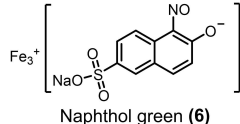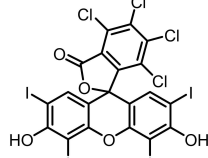### Re-oxidation to *para*-periodate using dye-containing solutions

The UV/Vis measurements were used to easily follow the degradation (Figures S3–S18) of different dyes present in the anodic compartment. For these experiments, a dye concentration of 1×10^{-4} M was used. This concentration proved to be ideal to direct measurements of UV/Vis without any type of dilution steps and with good sensitivity. To clarify that not only the fluorophore was degraded but a total degradation happened, high-resolution (HR)MS analyses were performed. Examples are displayed in the Supporting Information (section 14). The experiments were performed using the parameters displayed in Table 1.

Initially, aza dyes as sudan I (**1**), diamine green (**2**), and brilliant black (**3**) were added into the periodate platform oxidizer process. Figure 3 depicts the variation of aza dye concentrations by normalized absorbance as a function of time and the periodate equivalents generated during the process. For a complete sodium *para*-periodate synthesis, 10 F (8-electron oxidation of NaI and 2 F for side reactions) are required for 1 equivalent.[55]

The equivalents of periodate production for 90% degradation of aza dyes decreases in the following order: **1** < **3** < **2**. Compound **1** degrades faster than compounds **2** and **3**, requiring 2.4 kilo equiv. of *para*-periodate being co-produced. Diamine green (**2**) and brilliant black (**3**) took 3.7 and 3.0 kilo equiv. of *para*-periodate to degrade until 90%, respectively. To further demonstrate the versatility of periodate's self-cleaning process, different dye structures were tested next: fluorescein (**4**), methylene blue (**5**), naphthol green (**6**), rose bengal (**7**), and perylenetetracarboxylic dianhydride (PTCDA) (**8**). Figure 4 displays the variation of ionic dyes' concentrations **4**–**8** by normalized absorbance as a function of time and *para*-periodate equivalents.
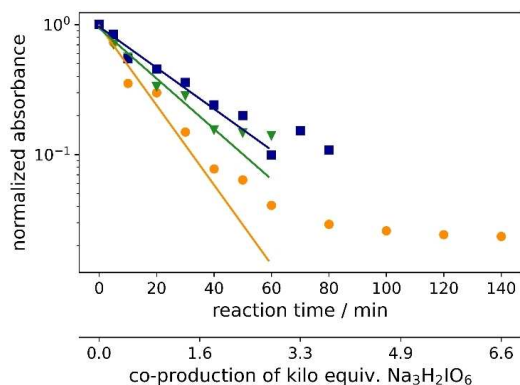
A 90% degradation of **4** corresponds to 1.6 kilo equiv. of *para*-periodate production. Ionic dyes like **5** and **6** were 90% decomposed within 26.2 and 2.9 kilo equiv. of *para*-periodate, respectively. The experiments with **7** and **8** took 8.2 and 18.8 kilo equiv. of *para*-periodate to be 90% degraded, respectively. Additionally, during the experiments with **7** and **8** we observed color variations in the degradation process, which could correspond to intermediate structures, formed during the re-oxidation process. This behavior made it difficult to fit such curves and follow the degradation by exponential fit equations. An image of the degradation process can be seen in the Supporting Information (Figures S16–S18). Considering the structure of the dyes in relation to the decomposition, a correlation between 90% degradation time and the compounds' structural nature could be confirmed. In general, more

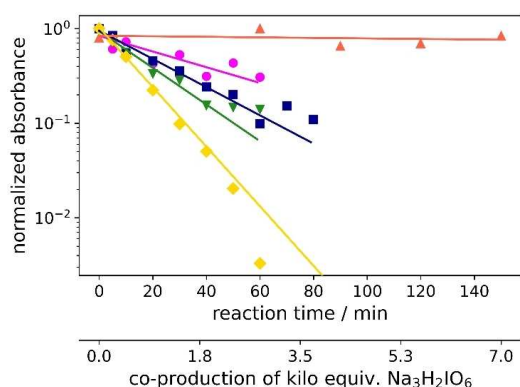**Table 1.** Electrochemical degradation of dyes in *para*-periodate platform oxidizer process.[a]

Dye (0.1 mM)	Degradation [kilo equiv. of $Na_3H_2IO_6$]		
	> 90%	> 95%	> 99%
Sudan I (**1**)	2.4	3.2	5.0
Diamine green (**2**)	3.7	4.8	7.4
Brilliant black (**3**)	3.0	4.0	6.2
Fluorescein (**4**)	1.6	2.0	3.1
Methylene blue (**5**)	26.2	34.1	52.4
Naphthol green (**6**)	2.9	3.7	5.8
Rose bengal (7)	the data was not fit by the exponential equation; formation of intermediate species (see Supporting Information)		
PTCDA (**8**)	the data was not fit by the exponential equation; formation of intermediate species (see Supporting Information)		

[a] reaction conditions: Flow electrolyzer (BDD|Nafion™ membrane| stainless steel, 4×12 cm^2 = 48 cm^2); dye (0.1 mM), NaOH (4 M), $Na_3H_2IO_6$ (0.21 M), H_2O (200 mL), $j = 312$ mA cm^{-2}, $Q = 6$–149 F, rt. Degradation determined by UV-*Vis* analysis. All the kilo equiv. of periodate were calculated as showed in the section 11 (Supporting Information).

electron rich compounds are more easily degraded than less electron rich ones.

ChemSusChem

Research Article
doi.org/10.1002/cssc.202200874

**Chemistry
Europe**
European Chemical
Societies Publishing

Figure 3. The degradation rate of the aza dyes brilliant black (blue ■), diamine green (green ▼), and sudan I (orange ●) during the electrochemical re-oxidation of *para*-periodate, $j = 312$ mA cm^{-2}, the flow rate was 7.5 L h^{-1}, in a divided flow electrolyzer. All UV/Vis spectra were recorded in caustic soda (0.21 M Na$_3$H$_2$IO$_6$, 4 M NaOH, 0.1 mM dye).

Figure 4. Kinetic degradation rate of the tested ionic dyes methylene blue (orange ▲), naphthol green (pink ●), brilliant black (blue ■), diamine green (green ▼), and fluorescein (yellow ♦) during electrochemical re-oxidation of para-periodate using UV/Vis data at a current density of 312 mA cm^{-2}, the flow rate of 7.5 L h^{-1}, in a divided flow electrolyzer. All UV/Vis spectra were recorded in caustic soda (0.21 M Na$_3$H$_2$IO$_6$, 4 M NaOH, 0.1 mM dye).

As illustrated in Table 1, we also compared the percentage of dye degradation in >95 and >99% with the equivalents of co-generated *para*-periodate. The results were derived from the respective exponential fit equations (Supporting Information, section 11). The equivalents of *para*-periodate follow the rationale mentioned above and depend on the electronic nature of each dye. More electron-rich dyes need less equiv. of *para*-periodate being co-generated, whereas electron-deficient ones need significantly more for the parallel occurring mineralization process. As an example, we can note the difference in equivalents necessary for the degradation of **1** (>95 and >99% using 3.2, and 5.0 kilo equiv. of *para*-periodate) compared with **5** (>95 and >99% using 34.1 and 52.4 kilo equiv). In this case, compound **5**, a more electron-deficient dye, needs 10 times more equiv. of *para*-periodate to be >99% degraded.

Re-oxidation to *para*-periodate using iodo, contrast, and chemotherapy agent-containing solutions

The degradation of iodine and chemotherapy agents was monitored using different analytical methods.[62] Methods with clear monitoring of degradation were used, according to each compound. Therefore, the concentration of each pharmaceutical had to vary to maintain a good sensibility of the respective detection. Regarding the experiments with diodrast (**9**), diatrizoate (**10**), and iohexol (**11**), liquid chromatography (LC)–MS was applied as analytic method and an initial concentration of 0.8 mM was used for these compounds. Details of the LC–MS analyses are provided in the Supporting Information (section 7). For fluorouracil (**12**), ^{1}H and ^{19}F (Figure S33a, b) nuclear magnetic resonance (NMR) spectroscopy and a concentration of 3 mM were used to identify the degradation.

Table 2 displays the results to contrast and chemotherapy agent degradation comparing with the equiv. of *para*-periodate.

Table 2. Electrochemical degradation of APIs in para-periodate platform oxidizer process.[a]

pharmaceutically active ingredients (API)	BDD ‖ Stainless steel $j = 312$ mA cm^{-2} divided flow cell $fr = 7.5$ L h^{-1} → CO$_2$ + H$_2$ + N$_2$ + H$_2$O + HF		
API (0.8–3 mM)	Degradation [kilo equiv. of Na$_3$H$_2$IO$_6$]		
	>90%	>95%	>99%
Diodrast (**9**)[b,c]	0.208	0.241	0.319
Diatrizoate (**10**)[b,c]	0.507	0.644	0.962
Iohexol (**11**)[b,c,d]	direct complete glycol cleavage in contact with anolyte solution		
Fluorouracil (**12**)[e,f]	0.056	0.072	0.110

[a] Reaction conditions: Flow electrolyzer (BDD ‖ Nafion membrane ‖ stainless steel, 4×12 cm^2 = 48 cm^2); dye (0.8–3 mM), NaOH (4 M), Na$_3$H$_2$IO$_6$ (0.21 M), H$_2$O (200 mL), 312 mA cm^{-2}, $Q = 9$–12 F, RT. All kilo equiv. of periodate were calculated as shown in section 11 (Supporting Information). [b] Concentration of 0.8 mM. [c] Degradation determined by LC–MS. [d] Degradation without electricity. [e] Concentration of 3 mM. [f] Degradation determined by ^{1}H NMR spectroscopy.
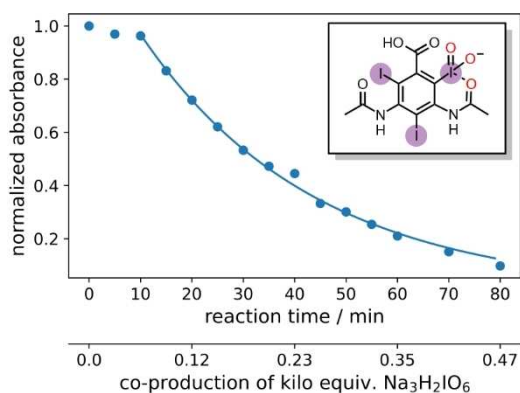
For >90, >95, and $>99\%$ degradation of **9**, 0.208, 0.241, and 0.319 kilo equiv. of $Na_3H_2IO_6$ production were necessary. On the other hand, **10** was >90, >95, and $>99\%$ degraded using 0.507, 0.644, and 0.962 kilo equiv. of *para*-periodate production. When **11** was subjected to the degradation process, the signal corresponding to this compound, observed by LC–MS, disappeared only in contact with the anolyte solution. In this case, immediate glycol cleavage occurs by the contact of basic/*para*-periodate solution, thus modifying the initial structure.

The LC–MS analyses were illustrated in the Supporting Information (Figures S60–S63). A further ^1H and ^{13}C NMR spectroscopic investigation indicated that the degradation process occurs in the alkyl chains, carbonyl, as well in the aromatic parts of the molecule. Probably, in the degradation process of the pharmaceuticals, halogen species are replaced by oxidative radicals formed at the anode. This is a comparably slow process. Thus, the more halogen atoms are present in the molecule, the more equiv. of *para*-periodate are necessary.[63,64] The first oxidation potentials of the APIs were measured using cyclic voltammetry, which support this hypothesis (Supporting Information, section 15).

Another factor that can cause a delay in the degradation process and increases the amount of necessary production of *para*-periodate is the possible formation of some interaction of *para*-periodate with the organic compounds. Thus, *para*-periodate can form intermediate complexes, which first need to cleave before the actual degradation can start.

As an example, the data analysis of **10** degradation is depicted (Figure 5). Here, we observed that the degradation of this compound starts with a delay, showing an exponential decay only after 10 min. This behavior can indicate a formation of some species as shown in the inset of Figure 5. Furthermore, the initial delay could be observed in other compounds as **9** and **12**. The degradation analyses of all the other investigated compounds can be found in the Supporting Information (Figures S40–S55).

Re-oxidation to *para*-periodate using iodo compound-containing solutions

Given the broad generality and operational simplicity of this degradation protocol triggered by *para*-periodate as platform oxidizer, we intended to explore the application of the methodology to late-stage diversification of versatile iodine compounds (see Table 3). Once again, different analytical methods as gas

Figure 5. UV/Vis analysis and proposed complex for the degradation of diatrizoate. The analysis was recorded in caustic soda (0.21 M $Na_3H_2IO_6$, 4 M NaOH, 0.8 mM diatrizoate).

Table 3. Electrochemical degradation of iodine compounds in *para*-periodate platform oxidizer process.[a]

Iodine compound (0.4–2 mM)	Degradation [kilo equiv. of $Na_3H_2IO_6$]		
	$>90\%$	$>95\%$	$>99\%$
Diiodomethane (**13a**)[b,c,d] → Iodomethanol (**13b**)[f]	direct degradation		0.25
Methyl 4-iodobenzoate (**14a**)[b,c,d] → 4-Iodobenzoic acid (**14b**)[d]	no further degradation of the carboxylic acid		
2-Iodobenzoic acid (**15**)[f,g]	0.136	0.176	0.271
3-Iodobenzoic acid (**16**)[f,d]	0.216	0.281	0.430
2-Iodoaniline (**17**)[f,h]	0.171	0.222	0.341
Dimethyl 5-iodoisophthalate (**18**)[f,g]	0.042	0.054	0.082
2,4,6-Triiodophenol (**19**)[f,h]	0.065	0.079	0.112

[a] Reaction conditions: Flow electrolyzer (BDD | Nafion membrane | stainless steel, 4×12 cm^2 = 48 cm^2); dye (0.4–2 mM), NaOH (4 M), $Na_3H_2IO_6$ (0.21 M), H_2O (200 mL), 312 mA cm^{-2}, Q = 0.5–23 F, RT. All kilo equiv. of periodate were calculated as showed in section 11 (Supporting Information). [b] Concentration of 0.4 mM. [c] Degradation without electricity. [d] Determined by ^1H NMR spectroscopy. [f] Concentration of 2 mM. [g] Determined by GC. [h] Determined by GC–MS.

ChemSusChem

Research Article
doi.org/10.1002/cssc.202200874

Chemistry
Europe

European Chemical
Societies Publishing

chromatography (GC), GC–MS and ^{1}H NMR spectroscopy were used to follow the degradation.

When diiodomethane (**13**) was employed to the re-oxidation within the *para*-periodate process, once being in contact with the anolyte solution the replacement of an iodine atom for a hydroxyl group can be observed, forming iodomethanol (**13b**). Over time, iodomethanol can form hydrate in equilibrium with formaldehyde, which can easily oxidize further under the given conditions.[65] But when methyl 4-iodobenzoate (**14**) was employed to the re-oxidation *para*-periodate process, we did not observe the degradation process. Instead, we observed the formation of 4-iodobenzoic acid (**14b**). Next, we investigated *ortho*- and *meta*-substituted iodobenzoic acids (**15** and **16**). For those compounds, >99% degradation was achieved using 0.271 and 0.430 kilo equiv. of *para*-periodate, respectively. The 2-iodoaniline (**17**) was tested and could be >90, >95, and >99% degraded using 0.171, 0.222, and 0.341 kilo equiv. of *para*-periodate. Nevertheless, dimethyl 5-iodoisophthalate (**18**) and 2,4,6-triiodophenol (**19**) were >99% degraded using surprisingly small amounts of *para*-periodate: 0.082 and 0.112 kilo equiv., respectively.

As shown in the previous and in this section, organic iodo compounds can be fed into the *para*-periodate generation for upcycling such iodo-containing waste into the platform oxidizer.

### Purity of *para*-periodate formed and influence of the pollutants

To clarify that after the re-oxidation process, we have *para*-periodate in high grade, LC–MS analysis was carried out after the degradation process. The results (Supporting Information, section 12) showed that after the process, the *para*-periodate has the same purity as before adding the organic contaminant into the anolyte compartment.

Thereafter, we could verify that we can electrochemically produce high-grade *para*-periodate using solutions containing organic molecules inside: We performed the following experiments, showed in Scheme 1.

In these cases, LC–MS analyses (Supporting Information) showed that formed $Na_3H_2IO_6$ exhibits the same purity grade than the *para*-periodate formed using Millipore water. The current efficiency (CE) for this experiment was 82% compared with 84% when the reaction was performed using Millipore water.

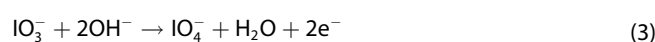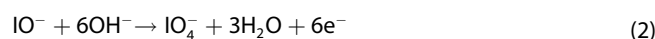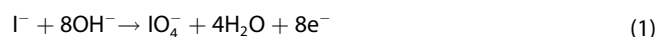### Role of hydroxyl radicals in the re-oxidation to *para*-periodate

In the periodate platform oxidizer process, dissolved unconverted iodine species are recycled within the anolyte, while *para*-periodate crystallizes during the process.[66–70] This means having a constant cycle of *para*-periodate production using unconverted iodine species.
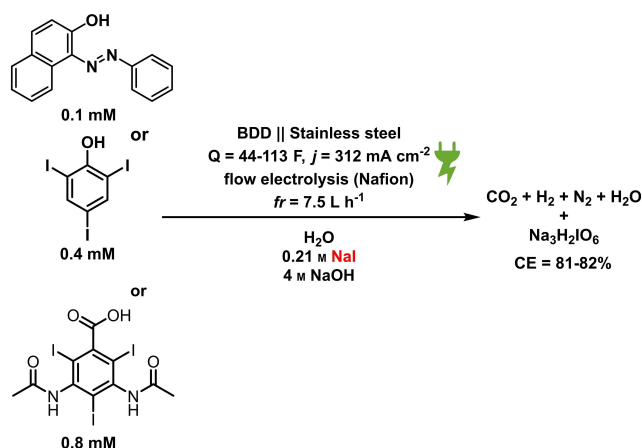
Scheme 1. Synthesis of *para*-periodate using solutions containing sudan I, 2,4,6-triiodophenol, and diatrizoate.

Regarding the theorical process analysis, 4 molecules of H_2O and 8 equiv. of hydroxide are consumed for the oxidation of 1 equiv. of iodine. 3 equiv. of H_2O and 6 equiv. of hydroxide are required for the oxidation of iodonium (I^+), which is generated by disproportion of I_2 requiring two additional equiv. of hydroxide for the formation of IO^-. One molecule of H_2O and 2 equiv. of hydroxide are required for the oxidation of iodate to periodate. In all cases, the same number of hydroxide equiv. is generated at the cathode. To form *para*-periodate from *meta*-periodate, only 2 equiv. of hydroxide are consumed. Among the electrochemical methods, anodic oxidation is driven by generated hydroxyl radicals.[55,67]

Equations (1)–(5) illustrate the process of formation and recycling of the *para*-periodate at the anode:

$$I^- + 8OH^- \rightarrow IO_4^- + 4H_2O + 8e^- \tag{1}$$

$$IO^- + 6OH^- \rightarrow IO_4^- + 3H_2O + 6e^- \tag{2}$$

$$IO_3^- + 2OH^- \rightarrow IO_4^- + H_2O + 2e^- \tag{3}$$

$$2H_2O \rightarrow 4H^+ + O_2 + 4e^- \tag{4}$$

$$IO_4^- + 2OH^- \rightarrow H_2IO_6^{3-} \tag{5}$$

Conclusion

We studied the influence of organic contaminations onto the regeneration of the electrochemical platform oxidizer *para*-periodate. It turned out that this re-oxidation to *para*-periodate results in a self-cleaning process due to the degradation of these organic compounds. Since the oxidation process at the anode is mediated by hydroxyl radicals, a concurrent mineralization of the organic entities occurs. The robustness of this platform process was demonstrated by contaminants consisting of dyes, active pharmaceutical ingredients, and organo-iodine compounds.

ChemSusChem

Research Article
doi.org/10.1002/cssc.202200874

**Chemistry
Europe**
European Chemical
Societies Publishing

In the concurrent degradation within the periodate process, we could observe a correlation between the electronic nature of the contaminant and the oxidation efficiency: Electron-rich contaminants are degraded first and need fewer equivalents of *para*-periodate being co-produced than less electron-rich compounds. Also, this strategy could degrade iodine compounds. Lastly, the iodo species can be recycled in the system for advanced *para*-periodate production.

To the best of our knowledge, this is the first example re-oxidizing *para*-periodate using contaminated water with organic molecules. This is the prerequisite for using periodate as a versatile platform oxidizer for sensitive applications, wherein the different streams for recycling may contain various contaminants. These are efficiently mineralized during the anodic process.

Experimental Section

The anodic compartment consists of the organic compound (0.1 mM for dyes, else 0.2–3 mM) and iodine sources, $NaIO_3$ or NaI (0.21 M) in caustic soda (32 g NaOH in 200 mL deionized water, 4 M). The cathodic compartment only contains caustic soda (4 M). The BDD anode and stainless-steel cathode, separated with a Nafion membrane, were connected to a galvanostat and both electrolytes were pumped (flow rate $= 7.5$ L h^{-1}) in cycling mode. A constant feed loop of catholyte to the anodic compartment was installed (flow rate $= 0.3$ mL min^{-1}). This was necessary to keep the volume of both compartments constant. The co-production of *para*-periodate ($j = 313$ mA cm^{-2}, Q as stated) was carried out at room temperature and the heat dissipated via a cryostatic bath circulator. Both compartments were stirred (300 rpm). The terminal voltage was 9.5 ± 0.5 V. For a reaction control, samples (2 mL) were taken in regular time steps, filtered over a glass frit to remove the access of *para*-periodate, and the permeate neutralized using $NaHSO_{4(aq)}$ (2 M). Then, the solution was measured using the adequate analysis technique.

Acknowledgements

Conflict of Interest

The authors declare no conflict of interest.

Data Availability Statement

The data that support the findings of this study are available in the supplementary material of this article.

[1] G. G. Botte, *Electrochem. Soc. Interface* **2014**, *23*, 49–55.
[2] F. B. Mainier, L. P. C. Monteiro, A. C. M. Rocha, R. J. Mainier, *A. J. E. R.* **2013**, *10*, 24–30.
[3] K. Scott, *Dev. Chem. Eng. Miner. Process.* **2008**, *1*, 71–117.
[4] D. Pollok, S. R. Waldvogel, *Chem. Sci.* **2020**, *11*, 12386–12400.
[5] A. Wiebe, T. Gieshoff, S. Möhle, E. Rodrigo, M. Zirbes, S. R. Waldvogel, *Angew. Chem. Int. Ed.* **2018**, *57*, 5594–5619; *Angew. Chem.* **2018**, *130*, 5694–5721.
[6] S. Möhle, M. Zirbes, E. Rodrigo, T. Gieshoff, A. Wiebe, S. R. Waldvogel, *Angew. Chem. Int. Ed.* **2018**, *57*, 6018–6041; *Angew. Chem.* **2018**, *130*, 6124–6149.
[7] X. Dong, J. L. Roeckl, S. R. Waldvogel, B. Morandi, *Science* **2021**, *371*, 507–514.
[8] S. P. Blum, T. Karakaya, D. Schollmeyer, A. Klapars, S. R. Waldvogel, *Angew. Chem. Int. Ed.* **2021**, *60*, 5056–5062; *Angew. Chem.* **2021**, *133*, 5114–5120.
[9] S. P. Blum, L. Schäffer, D. Schollmeyer, S. R. Waldvogel, *Chem. Commun.* **2021**, *57*, 4775–4778.
[10] M. Yan, Y. Kawamata, P. S. Baran, *Chem. Rev.* **2017**, *117*, 13230–13319.
[11] M. Dörr, M. M. Hielscher, J. Proppe, S. R. Waldvogel, *ChemElectroChem* **2021**, *8*, 2621–2629.
[12] T. Wirtanen, T. Prenzel, J.-P. Tessonnier, S. R. Waldvogel, *Chem. Rev.* **2021**, *121*, 10241–10270.
[13] J. L. Röckl, D. Pollok, R. Franke, S. R. Waldvogel, *Acc. Chem. Res.* **2020**, *53*, 45–61.
[14] L. Schulz, S. R. Waldvogel, *Synlett* **2019**, *30*, 275–286.
[15] S. R. Waldvogel, S. Lips, M. Selt, B. Riehl, C. J. Kampf, *Chem. Rev.* **2018**, *118*, 6706–6765.
[16] T. H. Meyer, I. Choi, C. Tian, L. Ackermann, *Chem* **2020**, *6*, 2484–2496.
[17] C. M. Kisukuri, V. A. Fernandes, J. A. C. Delgado, A. P. Häring, M. W. Paixão, S. R. Waldvogel, *Chem. Rec.* **2021**, *21*, 2502–2525.
[18] J. Seidler, J. Strugatchi, T. Gärtner, S. R. Waldvogel, *MRS Energy Sustainability#j.hofmann - 16.08.2017 11:12:13* **2020**, *7*, 42.
[19] D. Pletcher, R. A. Green, R. C. D. Brown, *Chem. Rev.* **2018**, *118*, 4573–4591.
[20] M. B. Plutschack, B. Pieber, K. Gilmore, P. H. Seeberger, *Chem. Rev.* **2017**, *117*, 11796–11893.
[21] S. B. Beil, D. Pollok, S. R. Waldvogel, *Angew. Chem. Int. Ed.* **2021**, *60*, 14750–14759; *Angew. Chem.* **2021**, *133*, 14874–14883.
[22] A. Lipp, M. Selt, D. Ferenc, D. Schollmeyer, S. R. Waldvogel, T. Opatz, *Org. Lett.* **2019**, *21*, 1828–1831.
[23] B. Gleede, M. Selt, R. Franke, S. R. Waldvogel, *Chem. Eur. J.* **2021**, *27*, 8252–8263.
[24] C. Gütz, V. Grimaudo, M. Holtkamp, M. Hartmer, J. Werra, L. Frensemeier, A. Kehl, U. Karst, P. Broekmann, S. R. Waldvogel, *ChemElectroChem* **2018**, *5*, 247–252.
[25] C. Gütz, A. Stenglein, S. R. Waldvogel, *Org. Process Res. Dev.* **2017**, *21*, 771–778.
[26] B. Gleede, M. Selt, C. Gütz, A. Stenglein, S. R. Waldvogel, *Org. Process Res. Dev.* **2020**, *24*, 1916–1926.
[27] N. Tanbouza, T. Ollevier, K. Lam, *iScience* **2020**, *23*, 101720.
[28] T. Noël, Y. Cao, G. Laudadio, *Acc. Chem. Res.* **2019**, *52*, 2858–2869.
[29] R. J.-R. Bednarz, C. Brauer, S. R. Waldvogel, *GIT Lab. J.* **2021**, *10*, 50–52.
[30] H. Li, C. P. Breen, H. Seo, T. F. Jamison, Y.-Q. Fang, M. M. Bio, *Org. Lett.* **2018**, *20*, 1338–1341.
[31] S. A. Snyder, *Angew. Chem. Int. Ed.* **2017**, *56*, 8045–8045; *Angew. Chem.* **2017**, *129*, 8157–8157.
[32] A. Sudalai, A. Khenkin, R. Neumann, *Org. Biomol. Chem.* **2015**, *13*, 4374–4394.
[33] P. Liu, B. Pang, S. Dechert, X. C. Zhang, L. B. Andreas, S. Fischer, F. Meyer, K. Zhang, *Angew. Chem. Int. Ed.* **2020**, *59*, 3218–3225; *Angew. Chem.* **2020**, *132*, 3244–3251.
[34] P. V. Chouthaiwale, P. U. Karabal, G. Suryavanshi, A. Sudalai, *Synthesis* **2010**, *22*, 3879–3882.
[35] L. Kraszkiewicz, M. Sosnowski, L. Skulski, *Tetrahedron* **2004**, *60*, 9113–9119.
[36] M. Zhou, R. H. Crabtree, *Chem. Soc. Rev.* **2011**, *40*, 1875–1884.
[37] B. Plietker, *Synthesis* **2005**, *15*, 2453–2472.
[38] K. Satyanarayana, K. Srinivas, V. Himabindu, G. M. Reddy, *Org. Process Res. Dev.* **2007**, *11*, 842–845.

[39] X. Wang, Y. Zeng, L. Sheng, P. Larson, X. Liu, X. Zou, S. Wang, K. Guo, C. Ma, G. Zhang, H. Cui, D. M. Ferguson, Y. Li, J. Zhang, C. C. Aldrich, *J. Med. Chem.* **2019**, *62*, 2305–2332.

[40] X. Gao, S. K. Woo, M. J. Krische, *J. Am. Chem. Soc.* **2013**, *135*, 4223–4226.

[41] G. Brauer, *Handbook of preparative inorganic chemistry, V2.*, Vol. 2. Elsevier, Amsterdam, **2012**.

[42] P. Galletti, G. Martelli, G. Prandini, C. Colucci, D. Giacomini, *RSC Adv.* **2018**, *8*, 9723–9730.

[43] H. Liimatainen, J. Sirviö, H. Pajari, O. Hormi, J. Niinimäki, *J. Wood Chem. Technol.* **2013**, *33*, 258–266.

[44] D. Kong, P. Wan, Y. Chen, Z. U. H. Khan, Y. Tang, *Int. J. Electrochem. Sci.* **2015**, *10*, 6422–6432.

[45] B. N. Grgur, M. M. Gvozdenović, J. S. Stevanović, B. Z. Jugović, Lj. T. Trišović, *Chem. Eng. J.* **2006**, *124*, 47–54.

[46] S. R. Waldvogel, B. Janza, *Angew. Chem. Int. Ed.* **2014**, *53*, 7122–7123; *Angew. Chem.* **2014**, *126*, 7248–7249.

[47] Y. Xia, Q. Dai, J. Chen, *J. Electroanal. Chem.* **2015**, *744*, 117–125.

[48] L. J. J. Janssen, M. H. A. Blijlevens, *Electrochim. Acta* **2003**, *48*, 3959–3964.

[49] Y. Aiya, S. Fujii, K. Sugino, K. Shirai, *J. Electrochem. Soc.* **1962**, *109*, 419–424.

[50] J. V. Macpherson, *Phys. Chem. Chem. Phys.* **2015**, *17*, 2935–2949.

[51] N. Yang, S. Yu, J. V. Macpherson, Y. Einaga, H. Zhao, G. Zhao, G. M. Swain, X. Jiang, *Chem. Soc. Rev.* **2019**, *48*, 157–204.

[52] S. R. Waldvogel, S. Mentizi, A. Kirste, *Boron-Doped Diamond Electrodes for Electroorganic Chemistry. In: Heinrich, M., Gansäuer, A. (Eds) Radicals in Synthesis III.*, Springer, Heidelberg, **2011**.

[53] S. Lips, S. R. Waldvogel, *ChemElectroChem* **2019**, *6*, 1649–1660.

[54] S. O. Ganiyu, E. V. Santos, C. A. Martínez-Huitle, S. R. Waldvogel, *Curr. Opin. Electrochem.* **2022**, *32*, 100903.

[55] S. Arndt, D. Weis, K. Donsbach, S. R. Waldvogel, *Angew. Chem. Int. Ed.* **2020**, *59*, 8036–8041; *Angew. Chem.* **2020**, *132*, 8112–8118.

[56] J. Klein, K. Alt, S. R. Waldvogel, *Adv. Sustainable Syst.* **2022**, *6*, 202270010.

[57] S. Arndt, B. Grill, H. Schwab, G. Steinkellner, U. Pogorevčnik, D. Weis, A. M. Nauth, K. Gruber, T. Opatz, K. Donsbach, S. R. Waldvogel, M. Winkler, *Green Chem.* **2021**, *23*, 388–395.

[58] M. Klein, S. R. Waldvogel, *Angew. Chem. Int. Ed.* **2021**, *60*, 23197–23201; *Angew. Chem.* **2021**, *133*, 23382–23387.

[59] Z. Wang, A. Berbille, Y. Feng, S. Li, L. Zhu, W. Tang, Z. L. Wang, *Nat. Commun.* **2022**, *13*, 130.

[60] A. S. Mramba, P. P. Ndibewu, L. L. Sibali, K. Makgopa, *Electroanalysis* **2020**, *32*, 2615–2634.

[61] Y. Jiang, H. Zhao, J. Liang, L. Yue, T. Li, Y. Luo, Q. Liu, S. Lu, A. M. Asiri, Z. Gong, X. Sun, *Electrochem. Commun.* **2021**, *123*, 106912–106932.

[62] A. Nowak, G. Pacek, A. Mrozik, *Rev. Environ. Sci. Bio/Technol.* **2020**, *19*, 337–354.

[63] G. Korshin, M. Yan, *Environ. Eng.* **2018**, *23*, 345–353.

[64] E. Hapeshi, A. Lambrianides, P. Koutsoftas, E. Kastanos, C. Michael, D. Fatta-Kassinos, *Environ. Sci. Pollut. Res. Int.* **2013**, *20*, 3592–3606.

[65] J. Clayden, N. Greeves, S. G. Warren, *Organic Chemistry*, Oxford Universiy Press, Oxford, **2012**.

[66] Y.-C. Lee, M.-J. Chen, C.-P. Huang, J. Kuo, S.-L. Lo, *Ultrason. Sonochem.* **2016**, *31*, 499–505.

[67] L.-H. Chia, X. Tang, L. K. Weavers, *Environ. Sci. Technol.* **2004**, *38*, 6875–6880.

[68] M. P. Shah, *Removal of Refractory Pollutants from Wastewater Treatment Plants*, CRC Press, Boca Raton, **2021**.

[69] X. Li, X. Liu, C. Lin, C. Qi, H. Zhang, J. Ma, *Chemosphere* **2017**, *181*, 609–618.

[70] X. Yu, M. Zhou, Y. Hu, K. G. Serrano, F. Yu, *Environ. Sci. Pollut. Res. Int.* **2014**, *21*, 8417–8431.